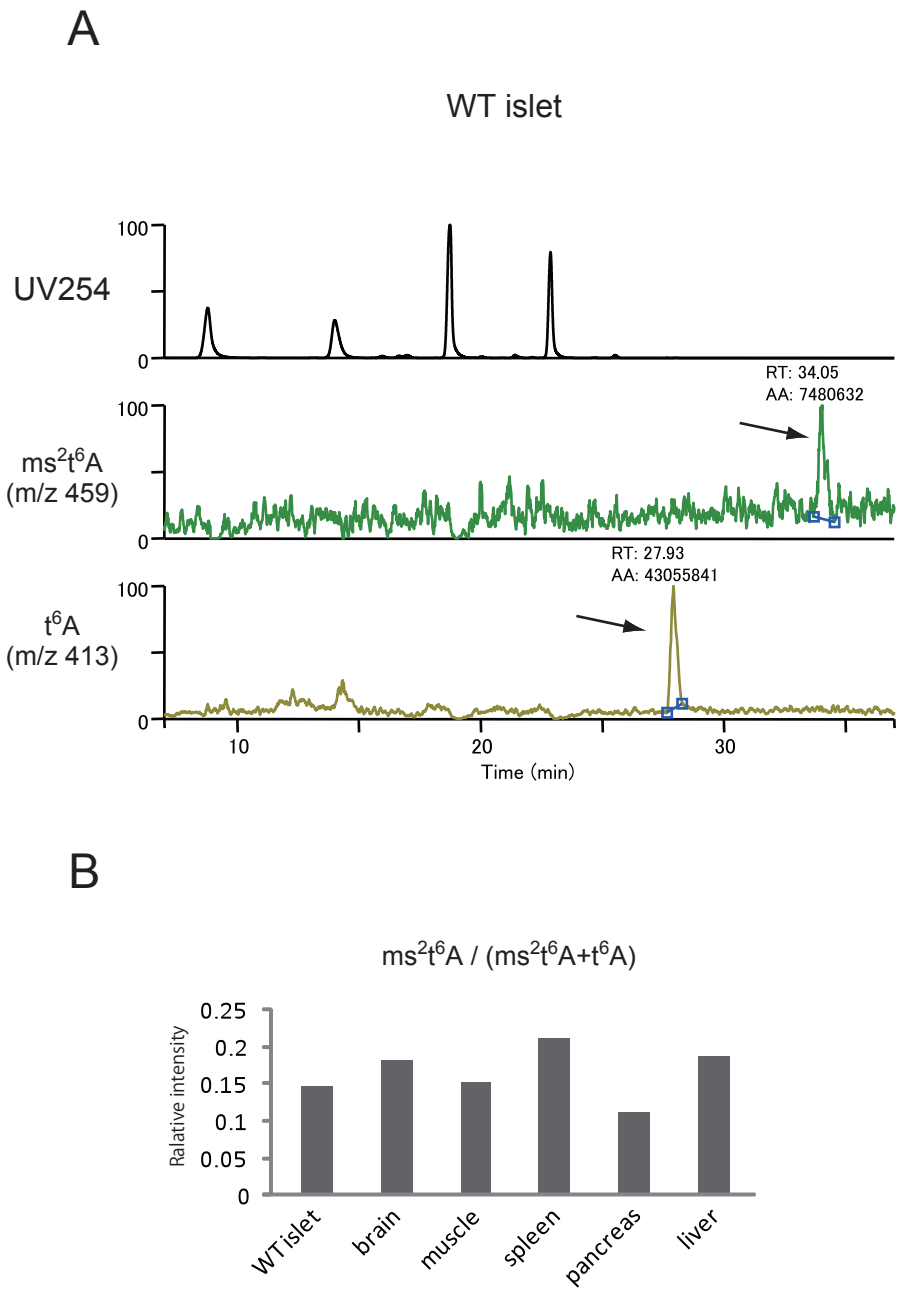

Supplemental Figure 1. Ubiquitous existence of the ms^2t^6A modification in mouse tissues. (A) Detection of the ms^2t^6Amodification in the pancreatic islets of WT mice. The upper panel shows the UV trace. The middle and lower panels show base peaks of mass chromatograms. Arrows indicate the peaks corresponding to ms^2t^6A (m/z 459) and t^6A (m/z 413), respectively. (B) RNA isolated from the indicated tissue was subjected to LC/MS. The relative amount of ms^2t^6 in each tissue was calculated by normalizing the peak area of ms^2t^6A to the sum of the peak areas of both ms^2t^6A and t^6A.

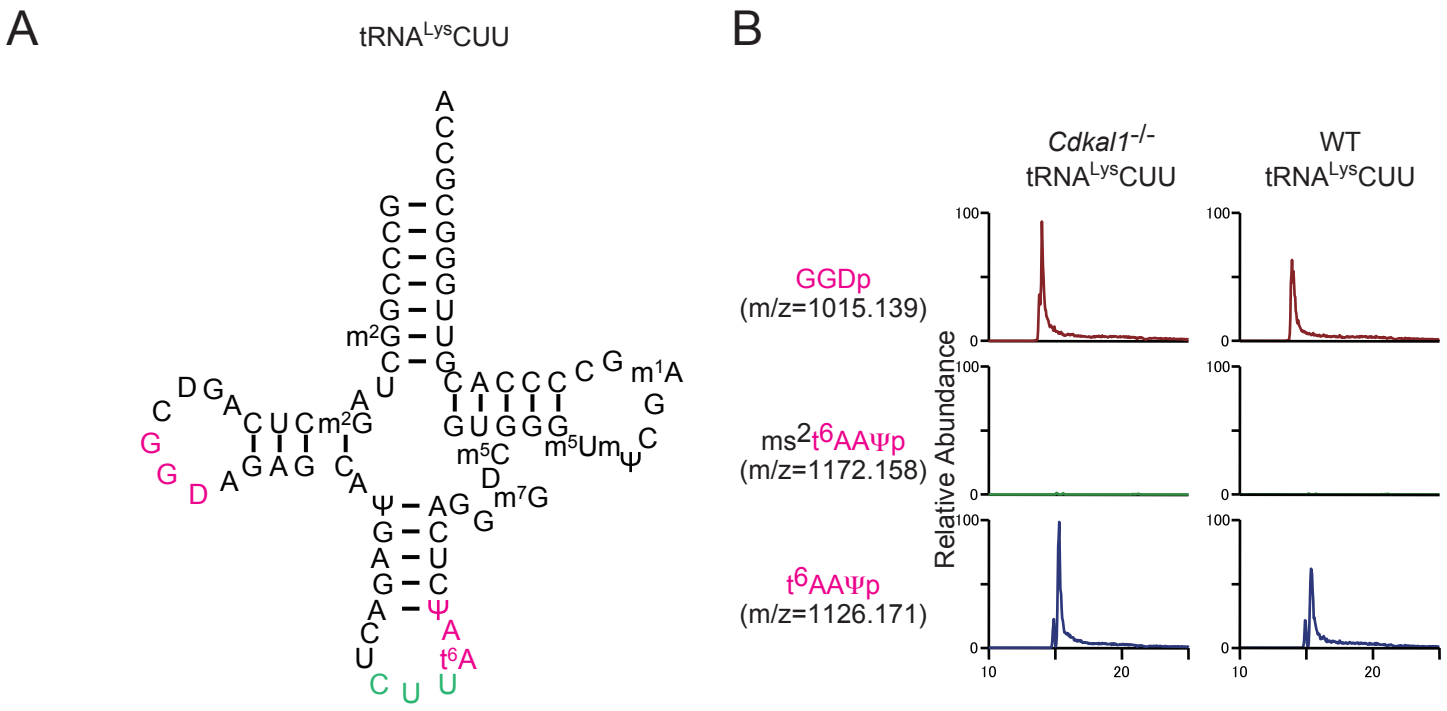

Supplemental Figure 2. Cdkal1 does not modify tRNA^{Lys}(CUU). (A) The secondary structure of mouse tRNA^{Lys}(CUU). Assignments of modifications except for ms^{2}t^{6}A were cited from Hayenga et al.(1). Red represents nucleic acid fragments measured by the mass spectrometric analyses in **Figure 1D** and **Supplemental Figure 2B.** Green represents the anti-codon of each tRNA. Abbreviations for modified bases are as follows: m^{2}G, N^2-methlyguanosine; D, dihydrouridine; Ψ, pseudouridine; mcm^{5}s^{2}U, 5-methoxycarbonylmethyl-2-thiouridine; m^{7}G, 7-methylguanosine; m^{5}C, 5-methylcytosine; m^{5}Um, 5,2'-O-dimethyluridine; m^{1}A, 1-methyladenosine (B) Modification of tRNA^{Lys}(CUU) isolated from the livers of *Cdkal1*$^{-/-}$ and wild-type mice. tRNA^{Lys}(CUU) was purified from each strain of mice and subjected to LC/MS. The panels show the mass chromatograms of GGDp, ms^{2}t^{6}AAΨp and t^{6}AAΨp fragments. Note that no ms^{2}t^{6}A modifications were found in tRNA^{Lys}(CUU) isolated from WT or *Cdkal1*$^{-/-}$ liver.

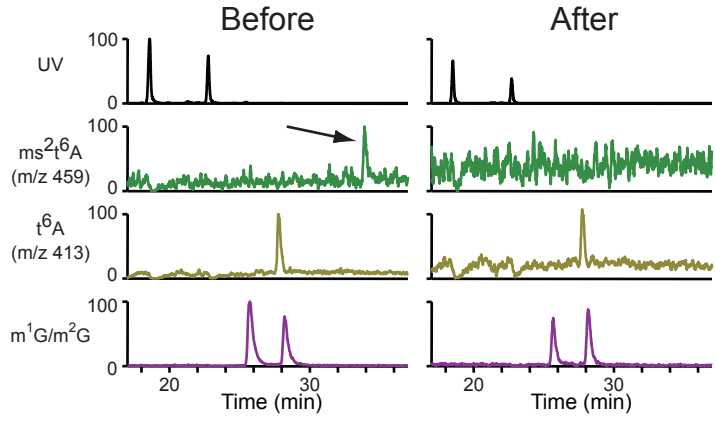

Supplemental Figure 3. The ms^2t^6A modification is exclusively found in $tRNA^{Lys}(UUU)$. The ms^2t^6A modification in crude tRNA and the flow-through fraction after affinity purification of $tRNA^{Lys}(UUU)$. The arrow indicates the peak corresponding to ms^2t^6A (m/z 459). The ms^2t^6A modification could not be detected after purification of $tRNA^{Lys}(UUU)$, indicating that it only exists in $tRNA^{Lys}(UUU)$.

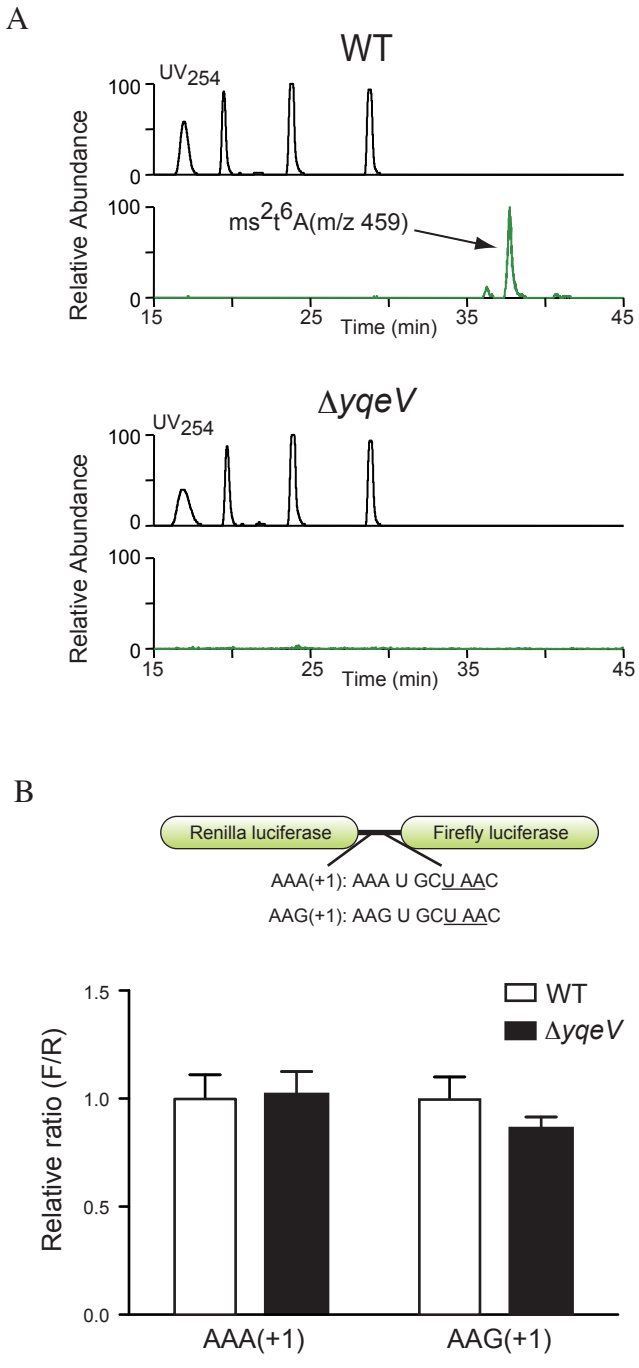

Supplemental Figure 4. Frame-shift assay of $tRNA^{Lys}$(UUU) in WT and Δ*yqe*Vbacillus subtilis. (A) Mass spectrometric analysis of the ms^2t^6A modification of tRNA in WT (upper pannels) and Δ*yqe*V (lower pannels) Bacillus subtilis. Arrow indicates ms^2t^6A (m/z 459). (B) Reporter constructs used to detect frame shifts during decoding of the AAA codon and AAG codon are shown. Reporter constructs consist of renilla luciferase, firefly luciferase, and a specific test sequence between them. The renilla luciferase is translated normally, whereas the firefly luciferase is only translated when a tRNA frame-shift occurs in the test sequence containing the AAA or AAG codon. If the frame-shift of $tRNA^{Lys}$(UUU) occurs during decoding of the AAA or AAG codon, firefly luciferase activity is increased. WT and Δ*yqe*V bacillus subtilis were transformed with the construct, and luciferase activity was measured. There were no differences in normalized firefly luciferase

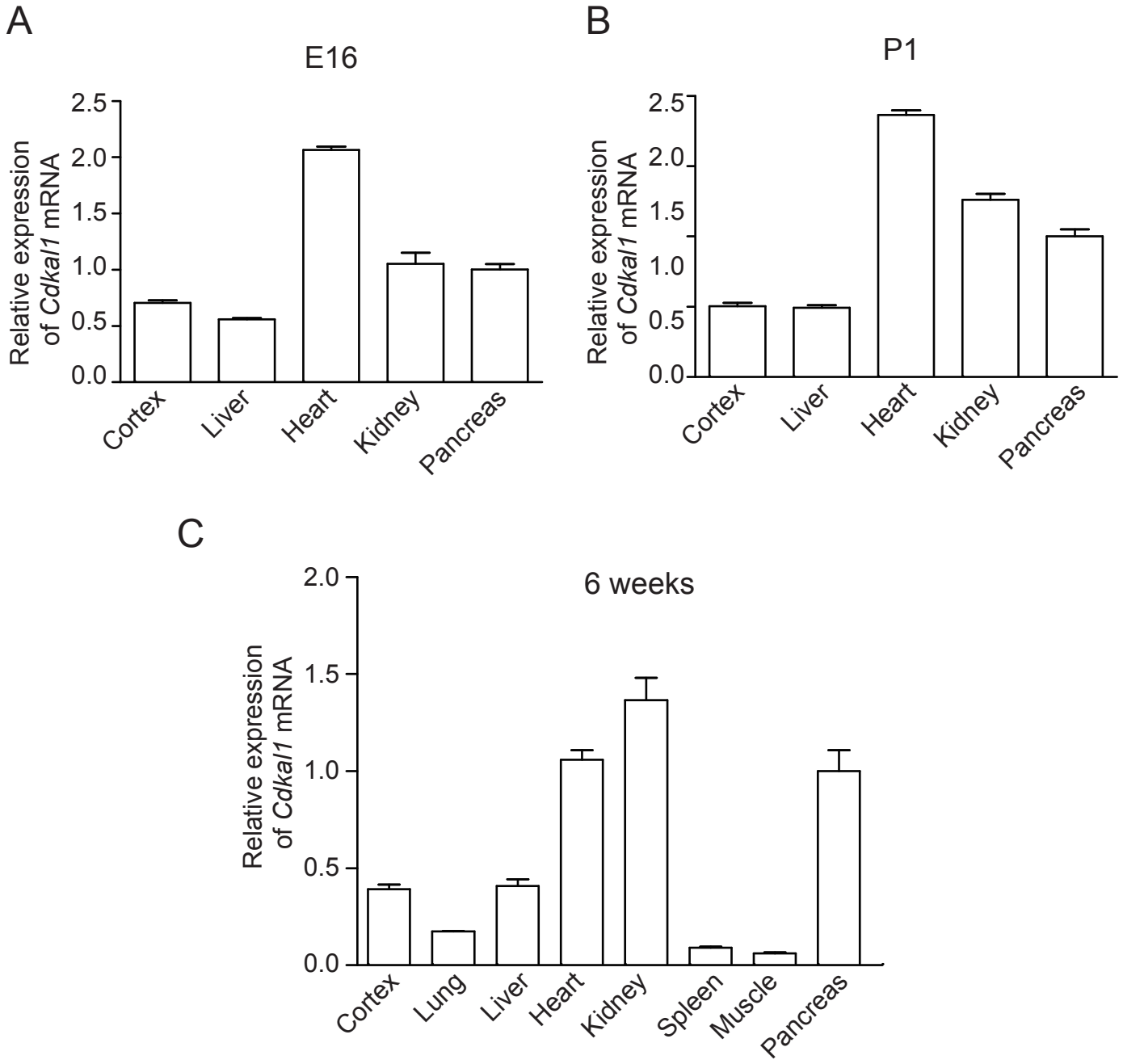

Supplemental Figure 5. Ubiquitous expression of the *Cdkal1* gene in mouse tissues. Total RNA was isolated from the indicated tissues at embryonic day 16 (A), postnatal day 1 (B), and 6 weeks (C). The level of *Cdkal1* mRNA was normalized to the level of β-actin.

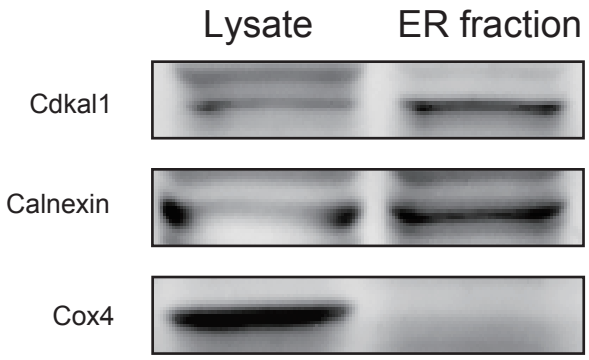

Supplemental Figure 6. Cdkal1 is localized to the ER. A rough ER-enriced fraction (ER fraction) was prepared from liver by calcium chloride precipitation using the ER isolation kit (Sigma). Proteins from whole liver lysate and the ER fraction was then loaded on a 4-12 % Tris-Glycine gel (Invitrogen). The expression of Cdkal1 was determined by Western blotting using anti-Cdkal1 antibody. Anti-Calnexin or anti-Cox4 antibody was used as a positive control for the ER and mitochodria, respectively. Note that there was no Cox4 signal in the ER fraction, indicating the fraction to be pure.

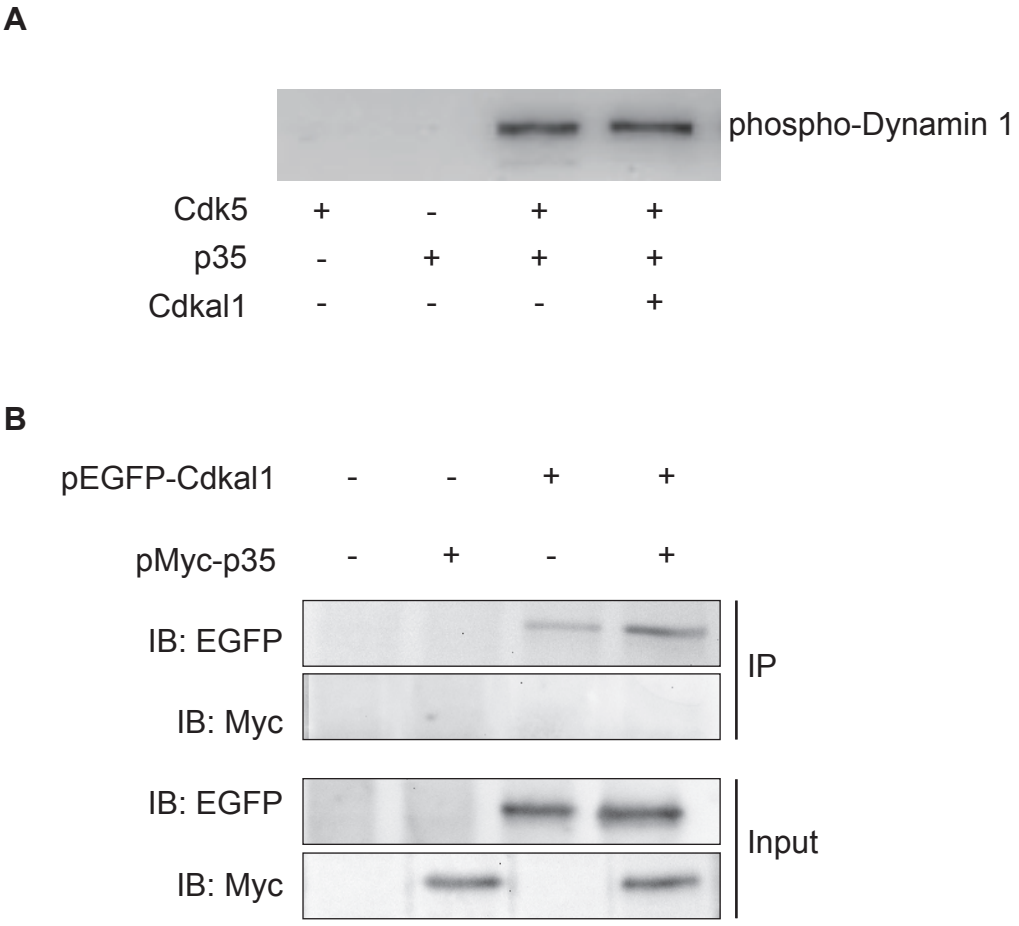

Supplemental Figure 7. Cdkal1 had no effect on Cdk5 activity or its interaction with p35. (A) Recombinant Cdk5/p35 was incubated with purified bovine dynamin 1, a physiological substrate of Cdk5, with or without recombinant GST-Cdkal1 for 30 min at 30 ºC. The reaction was terminated by adding 5x sample buffer and boiling for 5 min. Phosphorylated dynamin 1 was detected by western blotting using anti-phospho-dynamin 1 antibody (2). (B) Plasmids encoding EGFP-Cdkal1 and/or Myc-p35 were transfected into HEK293 cells. EGFP-Cdkal1 was immunoprecipitated by anti-EGFP antibody (MBL, Japan) conjugated on Dynabeads protein-A and released by boiling in 1x sample buffer. EGFP-Cdkal1 and Myc-p35 were detected by western blotting using anti-EGFP antibody (MBL) and anti-Myc antibody (Wako, Japan), respectively.

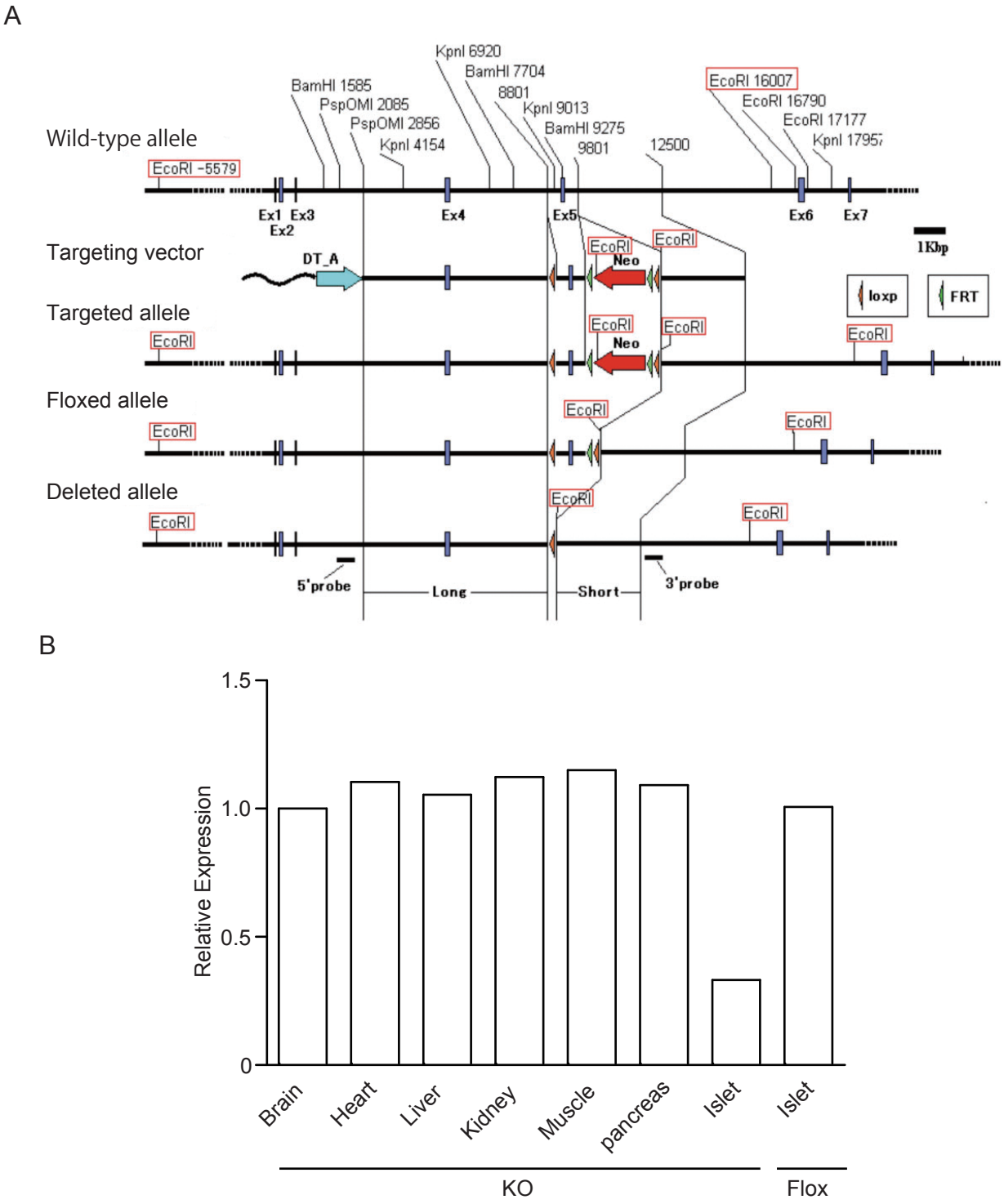

Supplemental Figure 8. Conditional knockout of *Cdkal1* in pancreatic β-cells. (A) The structure of the targeting vector for the generation of conditional *Cdkal1* transgenic mice. Exon 5 of *Cdkal1* gene was floxed by LoxP sequence to generate condtional *Cdkal1* KO mice (β cell KO mice). (B) Total RNA was isloated from brain, heart, liver, kidney, muscle, pancreas and islets of β cell KO mice (KO), and islets of Flox mice. Quantitative PCR (qPCR) was then performed to detect exon 5 in *Cdkal1* mRNA, which will be deleted after Cre-dependent recombination. Primers targeting exon 2-3 in *Cdkal1* mRNA were used for quantitative PCR as a control. The threshold cycle (Ct) number of qPCR targeting exon 5 was normalized to the Ct number of qPCR targeting exon 2-3. Note that exon 5 in *Cdkal1* was specifically deleted in pancretic islets of β cell KO mice, while it was intact in other tissues.

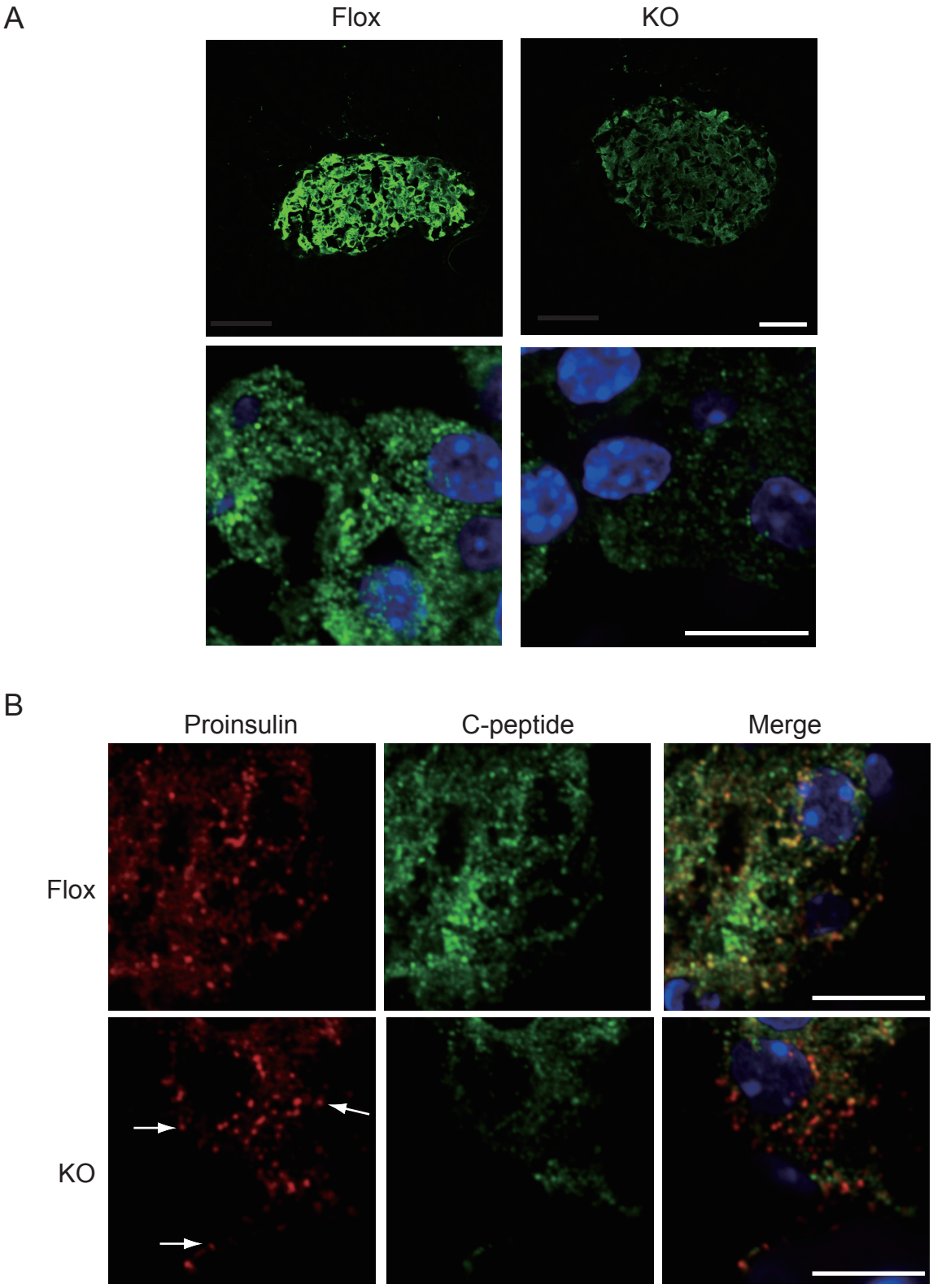

Supplemental Figure 9. Distinct targeting of proinsulin by Cdkal1 deficiency. (A) Pancretic islets of Flox and β cell KO mice (KO) were stained with anti-C-peptide antibody (Cell Signaling). The total intensity and the density of C-peptide positive granules was reduced in islets of Flox mice. Bar = 50 μm (upper), 10 μm (lower). (B) Pancreatic islets of Flox and β cell KO mice were stained with both anti-C-peptide and anti-proinsulin antibodies (Hytest). Note that there were proinsulin-positive granules which were not colocalized with C-peptide positive granules in islets of β cell KO mice. Bar = 10 μm.

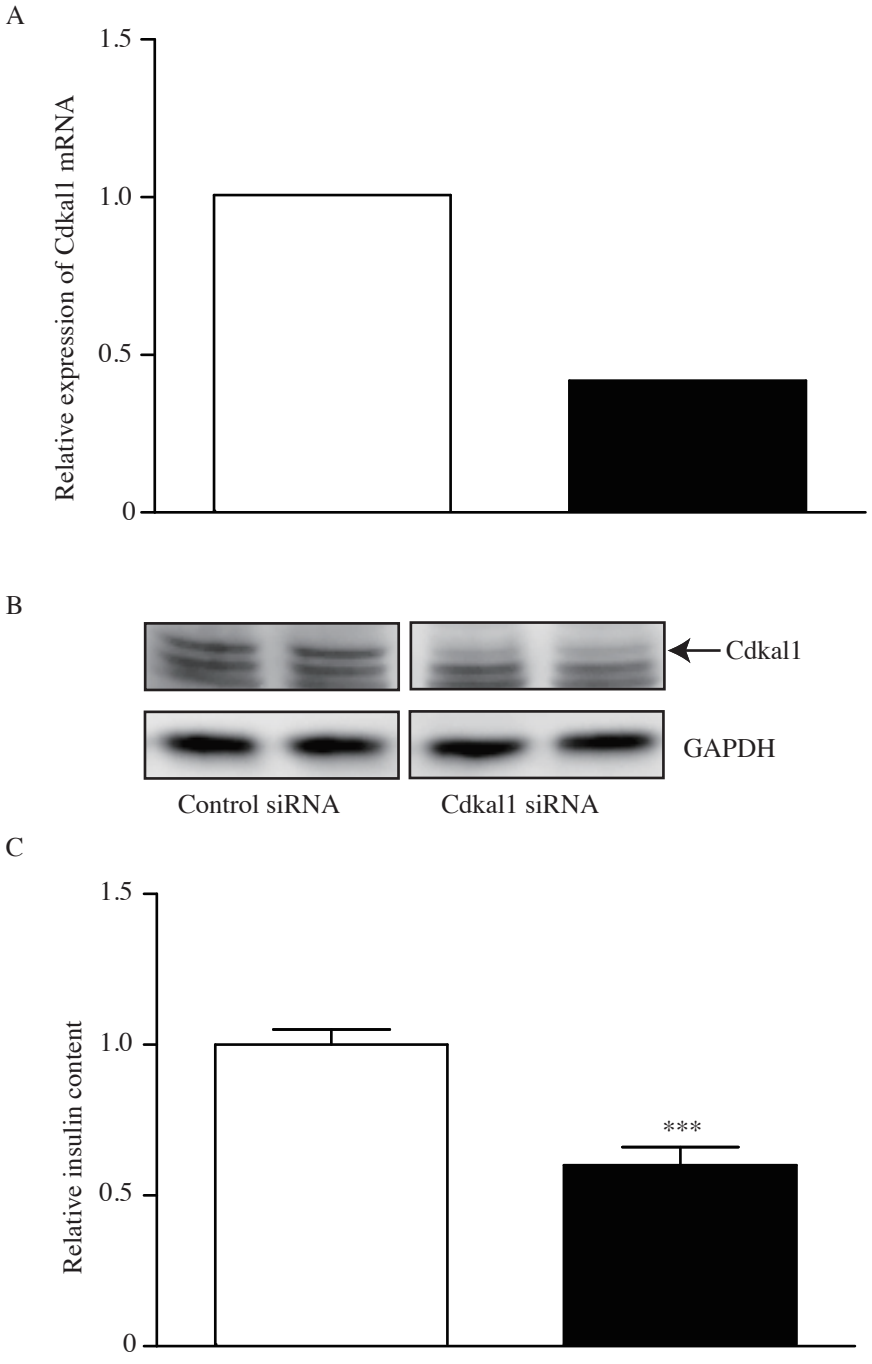

Supplemental Figure 10. Decrease of insulin content in MIN6 cells by knockdown of *Cdkal1*. (A) MIN6 cells were transfected with control siRNA or siRNA targeting mouse *Cdkal1* (Cdkal1 siRNA) mRNA by electroporation, and incubated for 72 h. The relative expression of *Cdkal1* mRNA to *GAPDH* mRNA was determined by quantitative PCR. The knockdown effeciency was 41% compared to the control. (B) Levels of Cdkal1 protein in MIN6 cells transfected with control siRNA or Cdkal1 siRNA for 72 hours determined by Western blotting. Note that there was a remarkable reduction of Cdkal1 protein level in MIN6 cells transfected with Cdkal1 siRNA. (C) Total insulin content of MIN6 cells transfected with control siRNA or Cdkal1 siRNA determined by ELISA. Note that there was a significant decrease in the amount of insulin in MIN6 cells transfected with Cdkal1 siRNA. n=6. ***$p<0.001$ Student' s *t* test.

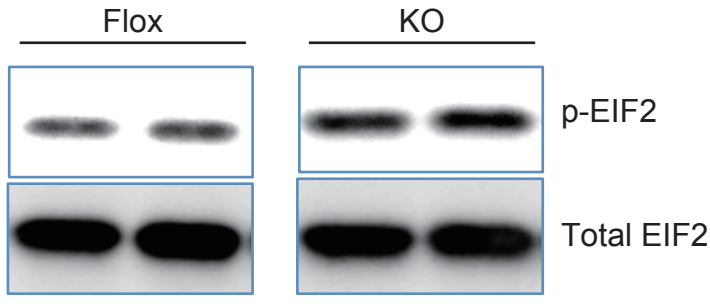

Supplemental Figure 11. Phospho-EIF2 levels in pancreatic islets of β cell KO mice and Flox mice. Islets isolated from either β cell KO mice (KO) or Flox mice were incubated in RPMI medium overnight. Fifty islets were incubated in KRB buffer containing 2.8 mM glucose for 30 minutes and homogenized in sample buffer. The levels of phospho-EIF2 and total EIF2 were examined by western blotting using anti-phospho-EIF2 and anti-EIF2 antibodies (Cell Signaling Technology).

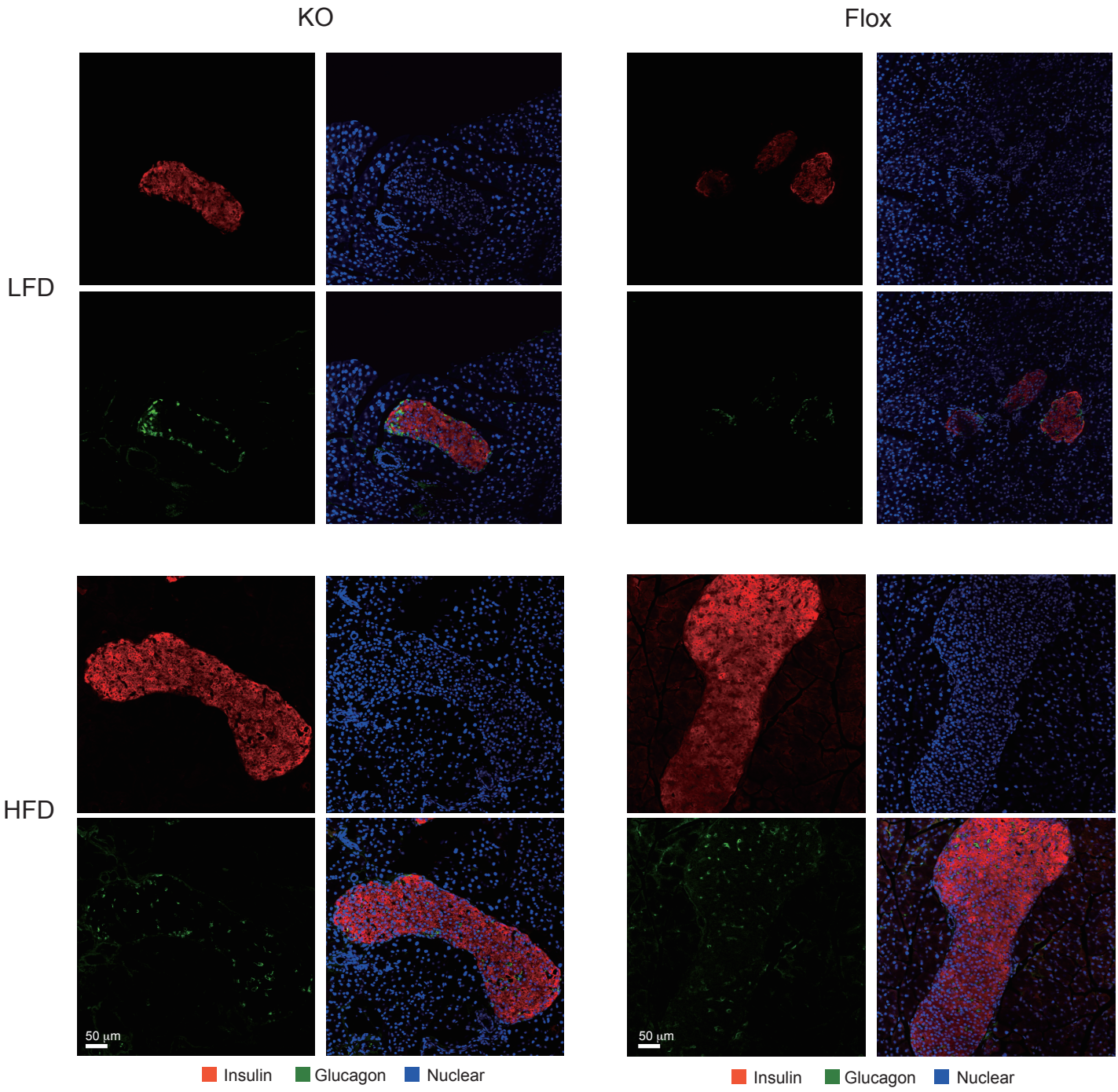

Supplemental Figure 12 A high-fat diet (HFD) induced pancreatic islet hypertrophy in both β cell KO and Flox mice. Both mice were fed an HFD for 9 weeks, and the pancreas was then removed. Frozen pancreatic sections were stained with anti-insulin antibody and anti-glucagon antibody. Hypertrophic islets were observed in both Flox mice and β cell KO mice (KO).

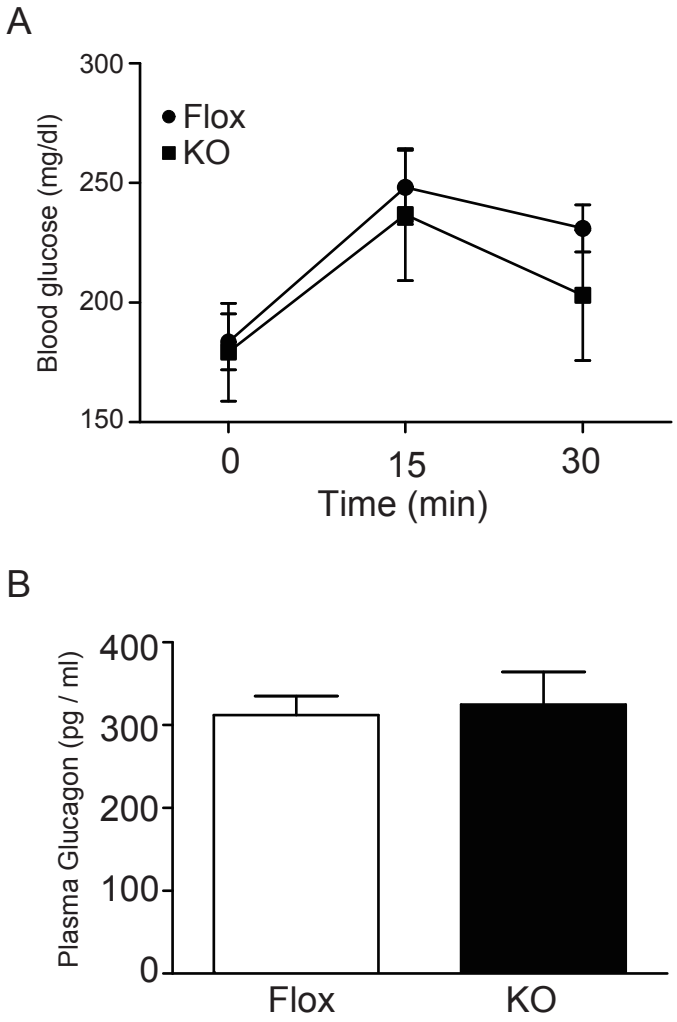

Supplemental Figure 13. Gluconeogenesis and Plasma glucagon levels in β cell KO mice. (A) β cell KO mice (KO) and Flox mice were fed an HFD for 10 weeks. Mice were fasted for 14 h and injected with 2g/kg sodium pyruvate. n=4-5. (B) Overnight-fasting plasma glucagon levels in Flox and β cell KO mice fed an HFD for 10 weeks. n=4-5.

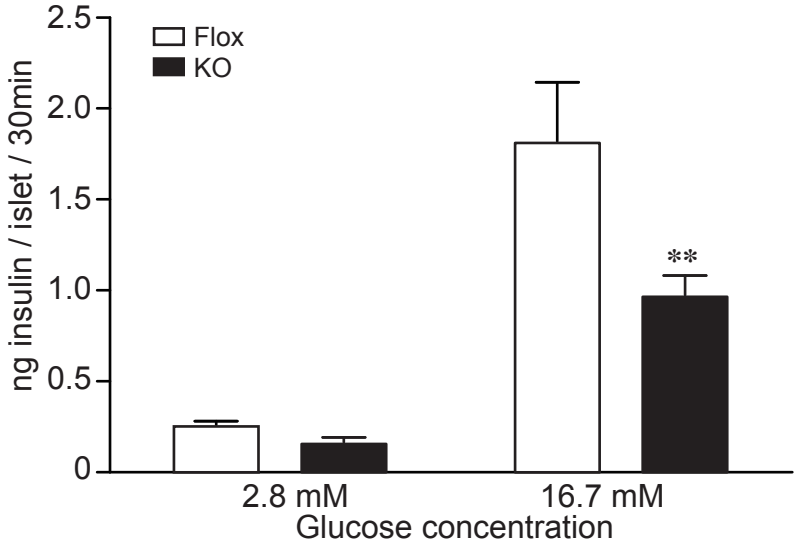

Supplemental Figure 14. Glucose-stimulated insulin secretion in the pancreas of Flox and β cell KO mice (KO) fed an HFD for 9 weeks. Mice were fed a high-fat diet for 9 weeks. Islets were then isolated from two or three mice and maintained in RPMI medium overnight. Ten islets were collected in test tubes and stimulated with either 2.8 mM glucose or 16.7 mM glucose for 30 min. The amount of insulin secreted from KO islets after treatment with 16.7 mM glucose was significantly lower than that secreted from Flox islets. n=8, **$P < 0.01$.

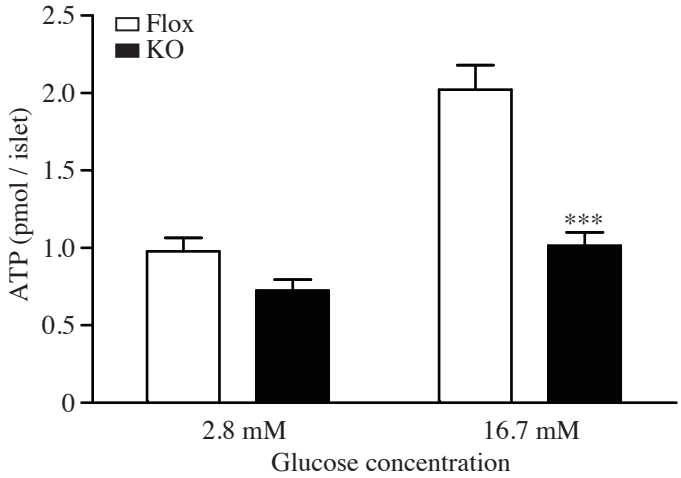

Supplemental Figure 15. Impaired glucose-stimulated ATP synthesis in islets of β cell KO mice. Islets isolated from Flox or β cell KO mice (KO) was incubated in RMPI medium overnight. Twenty five islets were preincubated in KRB buffer containing 2.8 mM glucose, and the buffer was replaced with fresh KRB buffer containing either 2.8 mM glucose or 16.7 mM glucose for 30 min. At the end of stimulation, the ATP in islets was extracted by adding boiling Tris buffer (100 mM Tris-HCl, pH 7.75, 4 mM EDTA). The ATP concentration was determined with an ATP Bioluminescence Assay Kit (Roche, Germany). Note that ATP synthesis after glucose treatment was significantly decreased in KO islets compared to Flox islets. n= 7-8. ***P<0.001, two-way ANOVA followed by Bonferroni posttest.

Gene name	5'	3'	Method
actin	GATCTGGCACCACACACCTTCT	GGGGTGTTGAAGGTCTCAAA	SYBR green
CHOP	CTGCCTTTCACCTTGGAGAC	CGTTTCCTGGGGATGAGATA	SYBR green
GLUT1	CAGTTCGGCTATAACACTGGTG	GCCCCCGACAGAGAAGATG	SYBR green
GLUT2	CAATTACCGACAGCCCATCC	TCCTGAGAACTGCTGGGCC	SYBR green
GLUT3	ATGGGGACAACGAAGGTGAC	GTCTCAGGTGCATTGATGACTC	SYBR green
XBP1-SPLICED	GAGTCCGCAGCAGGTG	GTGTCAGAGTCCATGGGA	SYBR green
XBP1-TOTAL	AAGAACACGCTTGGGAATGG	ACTCCCCTTGGCCTCCAC	SYBR green
ELF2	ACTTCGGGATTCACACATCC	GCCAATTCGGATCAGTTTGT	SYBR green
BIP	GGTGCAGCAGGACATCAAGTT	CCCACCTCCAATATCAACTTGA	SYBR green
Kir6.2	AAGGGCATTATCCCTGAGGAA	TTGCCTTTCTTGGACACGAAG	SYBR green
SUR1	TGAGCATTGGAAGACCCTCAT	CAGCACCGAAGATAAGTTGTCA	SYBR green
Glucokinase	AGGAGGCCAGTGTAAAGATGT	CTCCCAGGTCTAAGGAGAGAAA	SYBR green
MAFA	GCTGGTATCCATGTCCGTGC	GTCGGATGACCTCCTCCTTG	SYBR green
PDX1	GAGCGTTCCAATACGGACCA	TCAGCCGTTCTGTTTCTGGG	SYBR green
GADD34	CCCGAGATTCCTCTAAAAGC	CCAGACAGCAAGGAAATGG	SYBR green
Cdkal1	GCAAGCCACTGGCCAAGGGAG	AGCCAGGCCTGTAGCCACCT	SYBR green
Insulin 1	Mm01259683_g1		Taqman
Insulin 2	Mm00731595_gH		Taqman
Glucagon	Mm01269055_m1		Taqman
GAPDH	Part number: 4352932E		Taqman
Cdkal1	Mm0507443_m1		Taqman

Supplemental Table 1. Primer sequences used for quantitative PCR experiments.

Supplemental references

1. Hayenga K. et al. Structural relationship between tRNALys2 and tRNALys4 from mouse lymphoma cells. Mol. Cell Biochem. 1986; 71(1):25-30.

2. Tomizawa K. et al. Cophosphorylation of amphiphysin I and dynamin I by Cdk5 regulates clathrin-mediated endocytosis of synaptic vesicles. J. Cell Biol. 2003; 163(4):813-824.